

PAPER • OPEN ACCESS

Electron density and temperature diagnostics in laser-induced hydrogen plasma

To cite this article: G Gautam and C G Parigger 2017 *J. Phys.: Conf. Ser.* **810** 012055

View the [article online](#) for updates and enhancements.

Related content

- [Temperature diagnostics in a high-pressure hydrogen microwave plasma torch I: experimental characterization](#)
J Torres, E Iordanova, E Benova et al.
- [Influence of the laser pulse duration on plasma properties](#)
B Le Drogoff, J Margot, F Vidal et al.
- [Comparative Study on Excitation Temperature, Electron Temperature and Electron Density in an Atmospheric Argon Microwave Plasma](#)
Wang Zhong, Zhang Gui-Xin, Liu Cheng et al.



IOP | ebooks™

Bringing you innovative digital publishing with leading voices to create your essential collection of books in STEM research.

Start exploring the collection - download the first chapter of every title for free.

Electron density and temperature diagnostics in laser-induced hydrogen plasma

G Gautam and C G Parigger

University of Tennessee Space Institute, Center for Laser Applications, 411 B.H. Goethert Parkway, Tullahoma, TN 37388-9700, USA

E-mail: cparigge@tennessee.edu

Abstract. Laser-induced optical breakdown is achieved by using Q-switched, Nd:YAG radiation focused into ultra-high-purity (UHP) hydrogen gas at a pressure of $1.08 \pm 0.03 \times 10^5$ Pa inside a cell. The plasma emission spectra are dispersed by a Czerny-Turner type spectrometer and detected with an intensified charge-coupled device (ICCD). Stark-broadened hydrogen Balmer series H_α and H_β line profiles are used as a spectroscopic tool for the determination of electron density and excitation temperature. Spatial variation of electron density and temperature at 0.40 μ s are extracted from the recorded intensities of H_α and H_β lines. Temporal variations of electron density and excitation temperature are also presented for the time delay range of 0.15 μ s to 1.4 μ s.

1. Introduction

Hydrogen Balmer series lines have been explored in various theoretical and experimental investigations as well as tested experimentally to evaluate plasma parameters [1, 2]. Here, the Balmer series H_α and H_β lines are used for the electron density and excitation temperature diagnostics at various time delays. Figures 1 and 3 illustrate the electron density computed from the measured FWHM using Equation (1) [3]. These equations have been derived from previously collected data [4, 5],

$$N_{e,\alpha}[\text{cm}^{-3}] = \left[\frac{\Delta\lambda[\text{nm}]}{1.31} \right]^{1.56 \pm 0.07} \times 10^{17}, \quad N_{e,\beta}[\text{cm}^{-3}] = \left[\frac{\Delta\lambda[\text{nm}]}{4.50} \right]^{1.41 \pm 0.06} \times 10^{17}. \quad (1)$$

Electron excitation temperature is determined with the Boltzmann plot method [6] by utilizing the measured values of relative intensities of H_α and H_β lines. From these intensities, a straight line is plotted by applying the equation,

$$\ln \left[\frac{I_{ki}\lambda_{ik}}{g_k A_{ki}} \right] = - \left[\frac{E_k}{k_B T} \right] + \ln C, \quad (2)$$

where the following values are used [7]: Transition probabilities, $A_{ki} = 0.4410 \times 10^8 \text{ s}^{-1}$ and $0.08419 \times 10^8 \text{ s}^{-1}$, statistical weights, $g_k = 18$ and 32 , for H_α and H_β lines, respectively. Temperature values are computed from straight-line slopes. Intensity profiles of H_α and H_β lines along the lateral direction, *i.e.*, along the slit height, are used to determine the spatial variation of temperature.



2. Experiment

Micro-plasma is generated inside a cell containing 99.999% purity hydrogen gas by using Nd:YAG laser, operated at the fundamental wavelength of 1064 nm, frequency 10 Hz generating 13 ns pulses with an energy of 120 mJ. Spatially and temporally resolved plasma spectra are recorded with a Czerny-Turner type spectrometer and ICCD. A 1200 grooves/mm holographic grating is used to disperse the plasma emission into various wavelengths.

The ICCD consists of a 1024×1024 array with 1024 horizontal for wavelength and 1024 vertical pixels for intensity. In this experiment, eight vertical pixels are combined to reduce noise and improve the signal-to-noise ratio. A total of 128 lateral spectral measurements are possible along the slit height with this pixel binning. Each pixel is a square with $13.6 \mu\text{m}$ sides, therefore, each lateral measurement has a resolution of 0.1088 mm . The spectra recorded in the different zones indicate the variations of electron density and temperature.

A gate width of 20 ns is used for the time delay range of $0.15 \mu\text{s}$ to $1.4 \mu\text{s}$, and time steps of $0.25 \mu\text{s}$ are selected for the measurements of H_α and H_β emission spectra. Each collected spectrum corresponds to an average of 100 consecutive laser-plasma events.

3. Results

Spatial variations of an electron density, N_e , and temperature, T_e , for a time delay of $0.4 \mu\text{s}$ are displayed in Figures 1 and 2. The spatial distances indicated in Figs. 1 and 2 correspond to the slit height. The laser radiation propagates parallel to the slit, viz. from right to left.

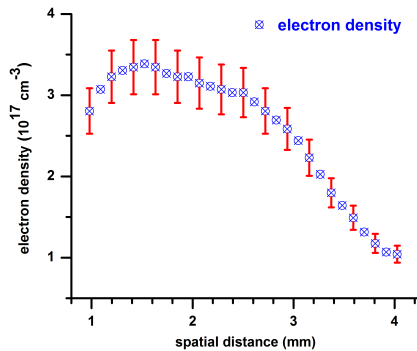


Figure 1. N_e variation from H_α , $0.4 \mu\text{s}$ time delay.

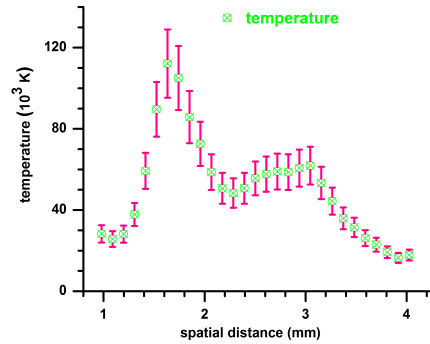


Figure 2. T_e variation from H_α , $0.4 \mu\text{s}$ time delay.

Full width at half maximum (FWHM) values are extracted from Lorentzian fits to the experimental data. Variation in FWHM values are found in the different zones of the plasma. This variation in FWHM values affects the electron densities due to approximately power of $3/2$ dependence in Eq. (1).

Spatial variations of N_e indicate up to a factor of 3 difference and an average value of $2.6 \times 10^{17} \text{ cm}^{-3}$ for a time delay of $0.4 \mu\text{s}$. The results of the spatial variation of electron density inferred from the H_β line are communicated in a recent article [8].

The spatial variation of temperature shows up to a factor of 7 difference with an average value of $52 \times 10^3 \text{ K}$. The estimated $\pm 15\%$ error bars used for temperature values are higher than $\pm 10\%$ error bars for electron density due to the increased uncertainties in determining temperatures.

Temporal variations of electron density and temperature determined from H_α and H_β lines are displayed in Figures 3 and 4. The electron densities agree with the line-of-sight values obtained from H_β lines [8] and are within the error bars of previous experiments in hydrogen gas [2, 4].

The measured plasma volume is represented by 29 values of the FWHM. At the time delay of 0.15 μs , incomplete line profiles of H_β cause increased error margins in the measured electron densities. The temporal electron density variations are in the range of $8 \times 10^{17} \text{cm}^{-3}$ to $0.5 \times 10^{17} \text{cm}^{-3}$ for time delays of 0.15 μs to 1.4 μs .

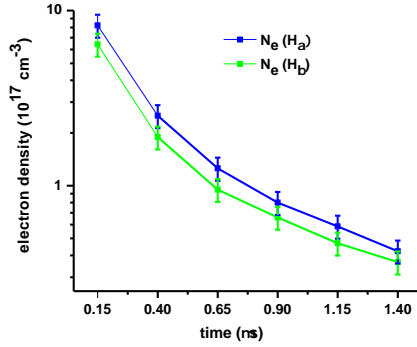


Figure 3. Temporal variation of electron density.

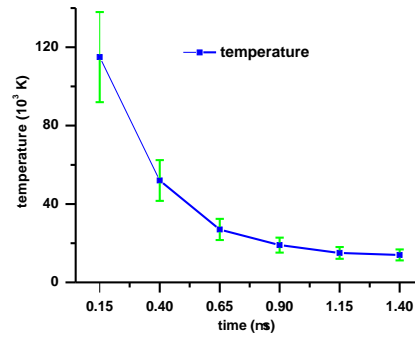


Figure 4. Temporal variation of excitation temperature.

The temperature changes decrease with time as indicated in Figure 4. The temperatures are in the range of $115 \times 10^3 \text{K}$ to $14 \times 10^3 \text{K}$ for time delays of 0.15 μs to 1.4 μs . These values are consistent with the previous hydrogen experiments [4]. Estimated error bars for electron density and excitation temperature are $\pm 15\%$ and $\pm 20\%$, respectively. The error bars for the temporal variation are slightly larger than for the spatial variation due to the use of a 20 ns gate width in the measurements reported here.

4. Conclusions

Recently derived empirical formulae are implemented for the electron density diagnostics. These formulae are applicable for the analysis of electron density in the indicated time delay range. Furthermore, both H_α and H_β lines can be used for the electron density diagnostics. The spatial variation of electron density and excitation temperature at 0.4 μs show up to a factor of 3 and 7 difference, respectively. Application of Abel inversion methods to extract radial distribution of electron density and excitation temperature is of continued interest.

Acknowledgments

The authors thank for support in part by the Center for Laser Applications at the University of Tennessee Space Institute.

References

- [1] Griem H R 1974 *Principles of Plasma Spectroscopy* (McGraw-Hill, New York)
- [2] Parigger C G 2013 *Spectrochim. Acta Part B* **79-80** 4
- [3] Surmick D M and Parigger C G 2014 *Int. Rev. At. Mol. Phys.* **5** 73
- [4] Parigger C G, Plemmons D H and Oks E 2003 *Appl. Opt.* **42** 5992
- [5] Parigger C G, Surmick D M, Gautam G and EL Sherbini A M 2015 *Opt. Lett.* **40** 3436
- [6] Wiese W L 1991 *Spectrochim. Acta Part B* **46** 831
- [7] Wiese W L and Fuhr J R 2009 *J. Phys. Ref. Data* **38** 565
- [8] Gautam G and Parigger C G 2014 *Int. Rev. At. Mol. Phys.* **5** 115